CrossMark

Codoping of Cr^{3+} in $Y_3Al_5O_{12}$:Ce^{3+} phosphors for improving color rendering of white light-emitting diodes

Yeqiu Wu[1] · Ziwei Chi[2] · Tao He[3]

Abstract A series of $Y_3Al_5O_{12}$:Ce^{3+}/Cr^{3+} phosphors were synthesized by a solid state reaction. $Y_3Al_5O_{12}$:Ce^{3+}/Cr^{3+} phosphors show emission bands in yellow and red regions corresponding to Ce^{3+} and Cr^{3+} ions. It was found that the emission intensity of Ce^{3+} decreases with the increasing Cr^{3+} concentration because of the energy transfer from Ce^{3+} to Cr^{3+} in $Y_3Al_5O_{12}$:Ce^{3+}/Cr^{3+} phosphors. The emission intensity of Cr^{3+} increases firstly and then decreases with the increasing Cr^{3+} concentration. The white light-emitting diode comprising of $Y_3Al_5O_{12}$:Ce^{3+}/Cr^{3+} phosphor shows a lower CCT value of 4452 and a higher R_a value of 85.7 than those of values of 6720 and 68.2 for white light-emitting diode comprising of $Y_3Al_5O_{12}$:Ce^{3+} phosphor.

1 Introduction

Light is needed in fields of industry and daily life. It has been reported that electric lighting covers up to ~25% of the average energy budget, and lighting and displays occupy ~20% of the electricity budget in the world [1]. White light-emitting diodes (WLEDs) show promise in a variety of eco-friendly and energy saving lighting applications in the general lighting and display fields because of their advantages over traditional incandescent or fluorescent lightings, such as high luminous efficiency, long persistence, energy saving and therefore environmental benefits [2–4]. Currently, the most used fabrication of WLED is to combine a blue InGaN chip with a yellow-emitting $Y_3Al_5O_{12}$:Ce^{3+} (YAG:Ce) phosphor. However, due to the absence of red emission in YAG:Ce phosphor excited by a blue InGaN chip, this type of WLEDs always show a low color rendering index ($R_a < 80$) and a high correlated color temperature (CCT > 6000 K) [5]. These drawbacks induce that it is inappropriate for applications in indoor lighting and full color displays. The general way to overcome theses drawbacks is to supplement red emission based on the excitation of blue InGaN chip.

Focusing on YAG:Ce phosphor, some ions are codoped to obtain red emission or lead to red shift of Ce^{3+} emission band. Lee et al. synthesized YAG:Ce^{3+}/Eu^{3+} phosphors and they found that the YAG:Ce^{3+}/Eu^{3+} phosphor presents a broad emission band in the green-yellow spectral region due to Ce^{3+}, as well as a sharp emission peak around 610 nm in the red spectral region due to Eu^{3+} [6]. Chen et al. synthesized YAG:Ce^{3+}/Gd^{3+} phosphors and they found that the emission peak of which can be regulated from approximately 543 nm to maximum 575 nm by tailoring the Gd^{3+} concentration until the collapse of crystal lattice [7]. Wang et al. synthesized YAG:Ce^{3+}/Cr^{3+} phosphors via conventional solid state reaction, which exhibits enriched emission spectrum in the red region due to a nonradiative energy transfer from Ce^{3+} to Cr^{3+} [8]. The existence of energy transfer between Ce^{3+} and Cr^{3+} means that tunable luminescence can be obtained by changing concentration ratios of Ce^{3+} and Cr^{3+}. This characteristic of YAG:Ce^{3+}/Cr^{3+} phosphor leads to the obtaining of tunable R_a and CCT for the fabricated WLEDs.

✉ Tao He
hetaowz@yeah.net

1 Department of Building Engineering, Shanxi Datong University, Datong 037003, People's Republic of China

2 Department of Power Engineering, School of Energy, Power and Mechanical Engineering, North China Electric Power University, Baoding 071003, People's Republic of China

3 Wenzhou Vocational and Technical College, Wenzhou 325003, People's Republic of China

In this work, we have synthesized a series of YAG:Ce^{3+}/Cr^{3+} phosphors through a solid state reaction. The luminescence, mechanism of energy transfer from Ce^{3+} to Cr^{3+} and chromaticity diagrams of YAG:Ce^{3+}/Cr^{3+} phosphors have been studied carefully. The performance of energy transfer leads to simultaneous observation of yellow emission from Ce^{3+} and deep red emission from Cr^{3+} upon blue light excitation. Moreover, performances of WLEDs encapsulated with YAG:Ce^{3+}/Cr^{3+} phosphor have been studied.

2 Experiment

YAG:4 mol%Ce^{3+}/xmol%Cr^{3+} (x = 0, 1, 2, 3, 4, 5 and 6) phosphors were synthesized by a solid state reaction. Y$_2$O$_3$ (99.99%), Al$_2$O$_3$ (99.99%), CeO$_2$ (99.99%) and Cr$_2$O$_3$ (99.99%) were used as raw materials. In the synthesis, raw materials with the stoichiometric proportions were weighted firstly. Then, the mixture was blended using a ball milling technique in ethyl alcohol media in a nylon bottle containing alumina balls for 10 h. Next, the slurry was dried at 80 °C for 12 h. Finally, the obtained powders were ground in an agate mortar and calcined at 1500 °C for 5 h in a reducing atmosphere of 5%H$_2$/95%N$_2$. After the system cooled to room temperature naturally, the product was ground again for further measurements.

The X-ray powder diffraction (XRD) measurements were carried out on a Rigaku-Dmax 2500 diffractometer using Cu Kα radiation (λ = 0.15405 nm). The excitation and emission spectra, as well as the decay of fluorescence of Ce^{3+} emission were measured by an Edinburgh Instrument FLS920 spectrophotometer equipped with a 150 W xenon lamp as the excitation source.

3 Results and discussion

Figure 1 shows the XRD patterns of YAG:4 mol%Ce^{3+} and YAG:4 mol%Ce^{3+}/4 mol%Cr^{3+} phosphors. All of diffraction peaks are well according with JCPDs No. 33-0040, demonstrating that the obtained phosphors have cubic phase and the Ce^{3+} and Cr^{3+} ions have doped into the lattices of YAG host. In YAG, Y atoms occupy the eight-coordinate oxygen atom dodecahedral site and Al atoms have two positions. The site of Al$_1$ is surrounded by six oxygen atoms resulting in an octahedral structure and the site of Al$_2$ is coordinated by four oxygen atoms to form a tetrahedral structure. Due to the same valence and similar ion radii between Y^{3+} (1.019 Å, CN = 8) with Ce^{3+} (1.143 Å, CN = 8) and Al^{3+} (0.53 Å, CN = 4; 0.675 Å, CN = 6) with Cr^{3+} (0.755 Å, CN = 6), Ce^{3+} is expected to substitute Y^{3+} site and Cr^{3+} is likely to substitute Al$_1$ site in YAG host. As shown in Fig. 1, the diffraction peaks shift to smaller 2θ
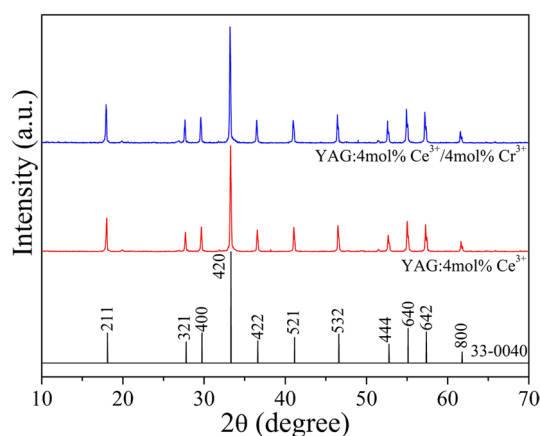
Fig. 1 XRD patterns of YAG:4 mol%Ce^{3+}, YAG:4 mol%Ce^{3+}/4 mol%Cr^{3+} phosphors and the standard data of JCPDs 33-0040
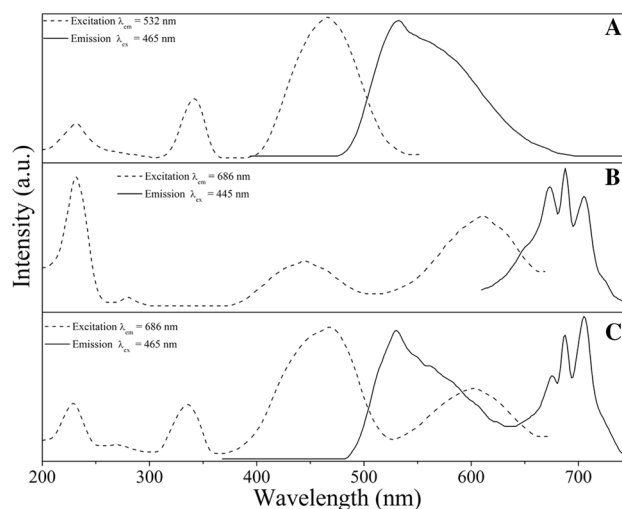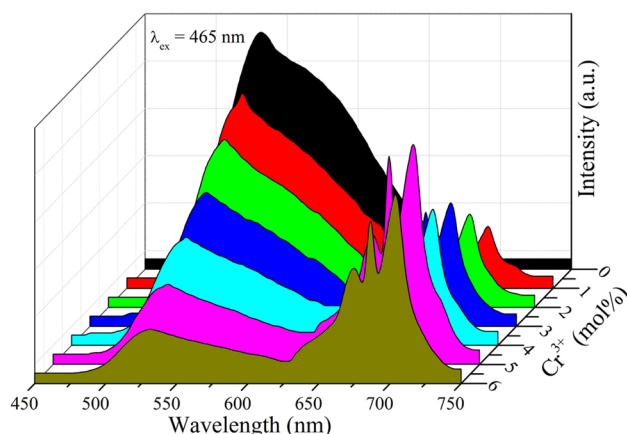

Fig. 2 Excitation and emission spectra of YAG:4 mol%Ce^{3+} (*a*), YAG:2 mol%Cr^{3+} (*b*) and YAG:4 mol%Ce^{3+}/4 mol%Cr^{3+} (*c*) phosphors

angels, which are induced by the larger radii of Ce^{3+} and Cr^{3+} than those of Y^{3+} and Al^{3+}.

Figure 2 presents the excitation and emission spectra of YAG:4 mol%Ce^{3+} (A), YAG:2 mol%Cr^{3+} (B) and YAG:4 mol%Ce^{3+}/4 mol%Cr^{3+} (C) phosphors. Ce^{3+} has only one electron in the 4f state. The ground state of Ce^{3+} is split into ^{2}F$_{7/2}$ and ^{2}F$_{5/2}$ with an energy difference of about 2200 cm^{-1} [9]. The next higher state originates from the 5d state and 4f–5d transitions are parity and spin allowed. For the free-ion, the 5d electron of the excited 4f^{1}5d^1 configuration forms a ^{2}D term, which is split into ^{2}D$_{3/2}$ and ^{2}D$_{5/2}$ states by spin–orbit coupling. Because that the radial wave function of the excited 5d electron extends spatially well beyond the closed 5s^{2}5p^6, its states

are strongly perturbed by the crystal field. Therefore, there are three excitation bands locating at 232, 341 and 465 nm in the excitation spectrum. The excitation band peaking at 232 nm is ascribed to the electron transition from ground state $4f$ to $5d$ sub-band energy level [10]. The band at 232 nm is very weak because the upper $5d$ states of Ce^{3+} in YAG have energies within the conduction band of the host. Therefore, excitation in these levels results mainly in quenching [11]. The excitation bands centering at 341 and 465 nm respectively correspond to the transitions from the ground state $4f$ levels ($^2F_{7/2}$, $^2F_{5/2}$) to the $5d_1$ and $5d_2$ levels [12]. The strongest excitation band peaking at 465 nm associates with the lowest-lying $5d$ state. The excitation band is deployed from the near-UV to the visible region. This means that the prepared phosphor is suitable for application in WLEDs excited by blue LED chip. Under the excitation at 465 nm, YAG:4 mol%Ce^{3+} shows a broad and asymmetric emission band ranging from 475 to 675 nm and peaking at 532 nm, which results from the $4f$–$5d$ transitions of Ce^{3+} ions. The emission band consists of doublet sub-emissions from $5d_1$ to $^2F_{2/7}$ and $5d_1$ to $2F_{5/2}$, because the ground state of Ce^{3+} consists of $^2F_{7/2}$ and $^2F_{5/2}$ sublevels after considering the spin–orbit interaction [13].

Figure 2b shows the excitation and emission spectra of YAG:2 mol%Cr^{3+} phosphor. In the excitation spectrum, an emission band peaking at 232 nm is a charge transfer band (CTB) relating to O^{2-}–Cr^{3+} [14]. The other three excitation bands peaking at 281, 445 and 611 nm can be ascribed to the spin-allowed electronic transitions of Cr^{3+} from the $^4A_2$ state to the $^4T_1$ (4 P), $^4T_1$ (4F) and $^4T_2$ (4F) states, respectively [15]. Under the excitation at 445 nm, YAG:2 mol%Cr^{3+} phosphor exhibits emission bands in the range of 600–750 nm, which are induced by the transitions form ^2E state to $^4A_2$ state [16]. For phosphors with sensitizer and activator, the effective energy transfer occurs when the emission spectrum of sensitizer overlaps with the excitation spectrum of activator [17]. From Fig. 2a, b, one can clearly see that there is an overlap between the emission band of YAG:4 mol%Ce^{3+} with the excitation band of YAG:2 mol%Cr^{3+}. Therefore, we can speculate that there is energy transfer from Ce^{3+} to Cr^{3+} in YAG:Ce^{3+}/Cr^{3+}. Figure 3c gives the excitation and emission spectra of YAG:4 mol%Ce^{3+}/4 mol%Cr^{3+} phosphor. By monitoring the emission at 686 nm, both excitation band of Ce^{3+} and excitation bands of Cr^{3+} are observed in the excitation spectrum. Under the excitation at 465 nm, the emission spectrum of YAG:4 mol%Ce^{3+}/4 mol%Cr^{3+} phosphor consists of a broad band in the yellow region and three emission bands in the red region, which respectively originate from Ce^{3+} and Cr^{3+}. The luminescence properties confirm the occurrence of energy transfer from Ce^{3+} to Cr^{3+} in YAG:Ce^{3+}/Cr^{3+}.

Fig. 3 Emission spectra of YAG:4 mol%Ce^{3+}/xmol%Cr^{3+} (x=0, 1, 2, 3, 4, 5 and 6) phosphors under the excitation at 465 nm
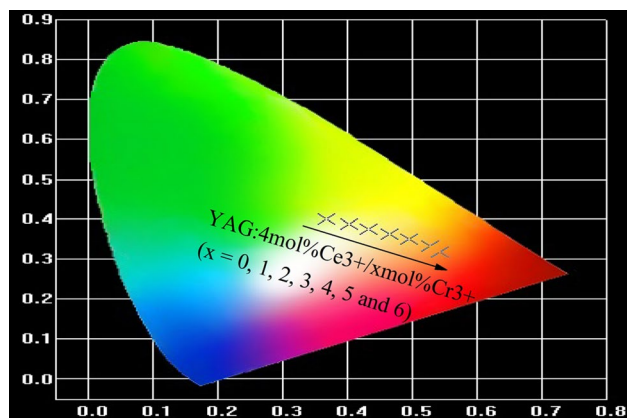
Fig. 4 CIE chromaticity coordinates of YAG:4 mol%Ce^{3+}/xmol%Cr^{3+} (x=0, 1, 2, 3, 4, 5 and 6) phosphors
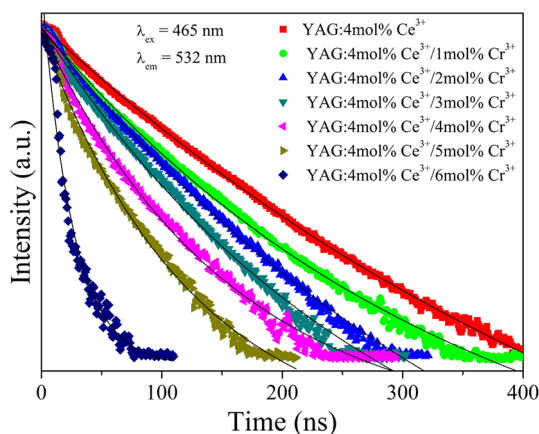
Figure 3 exhibits the emission spectra of YAG:4 mol%Ce^{3+}/xmol%Cr^{3+} (x=0, 1, 2, 3, 4, 5 and 6) phosphors under the excitation at 465 nm. The emission intensities show clear concentration-dependence. The emission intensity of Ce^{3+} decreases gradually with the increases of the Cr^{3+} concentration. The emission intensity of Cr^{3+} increases firstly with the increases of Cr^{3+} concentration and reaches a maximum at x=5. The emission intensity decreases if we further increase the Cr^{3+} concentration. The CIE chromaticity coordinates of YAG:4 mol%Ce^{3+}/xmol%Cr^{3+} (x=0, 1, 2, 3, 4, 5 and 6) phosphors are shown in Fig. 4 and Table 1. With the increases of Cr^{3+} concentration, the color of YAG:Ce^{3+}/Cr^{3+} phosphors changes from yellow region to yellow–red region. The variation of the emission spectra reveals the energy transfer process from Ce^{3+} to Cr^{3+} in YAG:Ce^{3+}/Cr^{3+} phosphors. And the decrease of Cr^{3+} emission intensity suggests the concentration quenching of Cr^{3+} for

Table 1 CIE chromaticity coordinates and energy transfer efficiencies of YAG:4 mol%Ce^{3+}/xmol%Cr^{3+} (x=0, 1, 2, 3, 4, 5 and 6) phosphors

Cr concentration (mol%)	CIE (x, y)		Energy transfer efficiency (η, %)	
	x	y	$\eta_{emission}$	η_{life}
0	0.367	0.400	/	/
1	0.403	0.388	13.50	12.77
2	0.432	0.375	22.12	24.21
3	0.465	0.362	32.98	32.46
4	0.496	0.351	41.24	41.52
5	0.527	0.332	50.17	51.24
6	0.543	0.317	58.46	58.53

YAG:4 mol%Ce^{3+}/6 mol%Cr^{3+} phosphor. The energy transfer efficiency ($\eta_{emission}$) from Ce^{3+} to Cr^{3+} can be calculated by the formula of $\eta = 1 - I_d/I_{d0}$, where I_d and I_{d0} are the luminescence intensity of Ce^{3+} in the presence and absence of the Cr^{3+} [18]. The values of $\eta_{emission}$ for YAG:4 mol%Ce^{3+}/xmol%Cr^{3+} (x=1, 2, 3, 4, 5 and 6) phosphors are shown in Table 1.

In order to further confirm the energy transfer from Ce^{3+} to Cr^{3+} in YAG:Ce^{3+}/Cr^{3+} phosphors, the decay curves of Ce^{3+} emission in YAG:4 mol%Ce^{3+}/xmol%Cr^{3+} (x=0, 1, 2, 3, 4, 5 and 6) phosphors have been measured by monitoring the Ce^{3+} emission at 532 nm. As shown in Fig. 5, the decay curves are well according with the single exponential function. The lifetimes of Ce^{3+} emission in YAG:4 mol%Ce^{3+}/xmol%Cr^{3+} (x=0, 1, 2, 3, 4, 5 and 6) phosphors are 40.32, 35.17, 30.56, 27.23, 23.58, 19.66 and 16.72 ns, respectively. The lifetimes of Ce^{3+} emission decrease with the increasing Cr^{3+} concentrations, which is

induced by the energy transfer from Ce^{3+} to Cr^{3+}. The energy transfer efficiency (η_{life}) also can be calculated by the following formula of $\eta = 1 - \tau/\tau_0$, where τ and τ_0 are the decay lifetimes of Ce^{3+} in the presence and absence of the Cr^{3+} [19]. The values of η_{life} for YAG:4 mol%Ce^{3+}/xmol%Cr^{3+} (x=1, 2, 3, 4, 5 and 6) phosphors are also shown in Table 1. The values of $\eta_{emission}$ and η_{life} are similar, which gives an accurate energy transfer efficiencies from Ce^{3+} to Cr^{3+} in YAG:4 mol%Ce^{3+}/xmol%Cr^{3+} (x=1, 2, 3, 4, 5 and 6) phosphors.

On the basis of the luminescent properties of YAG:Ce^{3+}/Cr^{3+} phosphors and the energy level diagrams of Ce^{3+} and Cr^{3+}, the mechanisms of emission and energy transfer have been speculated. Under the excitation of 465 nm light, electrons are excited to the 5d state from the 4f ground state. Most of excited electrons transfer back to the ground state and emit light in yellow region. The energy transfer from Ce^{3+} to Cr^{3+} in YAG:Ce^{3+}/Cr^{3+} phosphors occurs through two ways. As shown in Fig. 6, the ^2E energy level of Ce^{3+} is little higher than the $^4T_{2g}$ energy level of Cr^{3+}, which leads to the energy transfer through the nonradiative process [20]. The second way is that Cr^{3+} is excited from ground state of $^4A_2$ to the excited state of $^4T_2$ by absorbing the energy of emission light from Ce^{3+} ions [21]. However, we can see from Fig. 2b that Cr^{3+} is difficult to absorb energy of 532 nm light. Therefore, the first way of energy transfer is dominating.

To validate the availability of the synthesized phosphors for the InGaN based WLED, the WLEDs have been fabricate by combining the InGaN blue chip with the synthesized YAG:4 mol%Ce^{3+} and YAG:4 mol%Ce^{3+}/4 mol%Cr^{3+} phosphors. Figure 7 presents the electroluminescence spectra of WLEDs comprising of YAG:4 mol%Ce^{3+} (A) and YAG:4 mol%Ce^{3+}/4 mol%Cr^{3+} (B) phosphors under 20 mA current excitation. The spectrum of WLED based

Fig. 5 Decay curves of YAG:4 mol%Ce^{3+}/xmol%Cr^{3+} (x=0, 1, 2, 3, 4, 5 and 6) phosphors
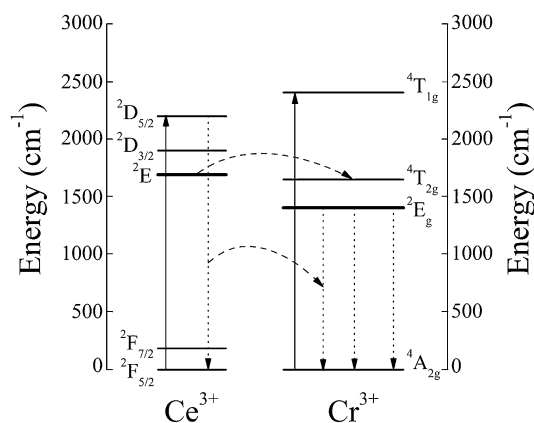
Fig. 6 Schematic energy level diagrams of Ce^{3+} and Cr^{3+} illustrating energy transfer process
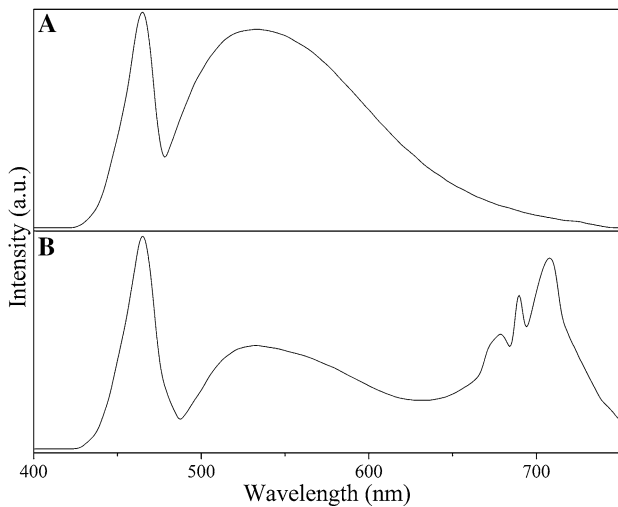
Fig. 7 Electroluminescence spectra of WLEDs comprising of YAG:4 mol%Ce^{3+} (*a*) and YAG:4 mol%Ce^{3+}/4 mol%Cr^{3+} (*b*) phosphors under 20 mA current excitation

on InGaN blue chip and YAG:4 mol%Ce^{3+}/4 mol%Cr^{3+} phosphor includes emission bands in blue, yellow and red regions. The blue emission band originates from the InGaN blue chip. The yellow emission band is induced by the YAG:Ce^{3+} under the excitation of InGaN blue chip. The red emission bands are ascribed to the Cr^{3+} ions in YAG:Ce^{3+}/Cr^{3+} phosphor under the excitation of InGaN blue chip. The mixture of blue–yellow–red light results in the generation of white light. The CIE chromaticity coordinates of WLEDs without and with codoping Cr^{3+} ions are (0.312, 307) and (0.348, 0.289), respectively. The values of CCT decrease from 6720 to 4452 and the values of R_a increase from 68.2 to 85.7 by the addition of Cr^{3+} in YAG:Ce^{3+} phosphor.

4 Conclusion

We have synthesized a series of YAG:Ce^{3+}/Cr^{3+} phosphors by a solid state reaction. The synthesized YAG:Ce^{3+}/Cr^{3+} phosphors show emission bands in yellow and red regions corresponding to Ce^{3+} and Cr^{3+} ions. Tunable luminescence is obtained in YAG:Ce^{3+}/Cr^{3+} phosphors by changing

Cr^{3+} concentration. The energy transfer from the ^2E energy level of Ce^{3+} to the $^4T_{2g}$ energy level of Cr^{3+} through non-radiative transition is dominating in YAG:Ce^{3+}/Cr^{3+} phosphor. The codoping Cr^{3+} in YAG:Ce^{3+} phosphor can decrease the CCT value and increase R_a value of WLED. The WLED comprising of YAG:Ce^{3+}/Cr^{3+} phosphor shows a lower CCT value of 4452 and a higher R_a value of 85.7 than those of values of 6720 and 68.2 for WLED comprising of YAG:Ce^{3+} phosphor.

References

1. Z. Xia, Q. Liu, Prog. Mater. Sci. **84**, 59 (2016)
2. S. Nakamura, Science **281**, 956 (1998)
3. B. Wang, Z. Xu, Z. Wang, C. Yang, J. Mater. Sci. **27**, 8183 (2016)
4. Y. Miao, P. Wang, H. Guan, Y. Chen, J. Mater. Sci. **27**, 10798 (2016)
5. H.S. Jang, Y.H. Won, D.Y. Jeon, Appl. Phys. B **95**, 715 (2009)
6. J.W. Lee, J.H. Lee, E.J. Woo, H. Ahn, J.S. Kim, C.H. Lee, Ind. Eng. Chem. Res. **47**, 5994 (2008)
7. L. Chen, X. Chen, F. Liu, H. Chen, H. Wang, E. Zhao, Y. Jiang, T.S. Chan, C.H. Wang, W. Zhang, Y. Wang, S. Chen, Sci. Rep. **5**, 11514 (2015)
8. W. Wang, J. Tang, S.T. Hsu, J. Wang, B. Patrick Sullivan, Chem. Phys. Lett. **457**, 103 (2008)
9. R.R. Jacobs, W.F. Krupke, M.J. Weber, Appl. Phys. Lett. **33**, 410 (1978)
10. J. Ueda, K. Kuroishi, S. Tanabe, Appl. Phys. Lett. **104**, 101904 (2014)
11. D. Haranath, H. Chander, P. Sharma, S. Singh, Appl. Phys. Lett. **89**, 173118 (2006)
12. Q. Li, L. Gao, D. Yan, Mater. Chem. Phys. **64**, 41 (2000)
13. P.A. Tanner, L. Fu, L. Ning, B.M. Cheng, M.G. Brik, J. Phys. **19**, 216213 (2007)
14. L. Wang, X. Zhang, Z. Hao, Y. Luo, X.J. Wang, J. Zhang, Opt. Express **18**, 25177 (2010)
15. R. Ma, C. Ma, J. Zhang, J. Long, Z. Wen, X. Yuan, Y. Cao, Opt. Mater. Express **7**, 454 (2017)
16. L.M. Shao, X.P. Jing, J. Lumin. **131**, 1216 (2011)
17. Y. Yang, B. Liu, Y. Zhang, X. Lv, L. Wei, X. Wang, Superlattices Microstruct. **90**, 227 (2016)
18. N. Guo, Y. Huang, M. Yang, Y. Song, Y. Zheng, H. You, Phys. Chem. Chem. Phys. **13**, 15077 (2011)
19. Y. Cao, N. Liu, J. Tian, X. Zhang, Polyhedron **107**, 78 (2016)
20. L. Hou, S.B. Cui, Z.L. Fu, Z.J. Wu, X.H. Fu, J.H. Jeong. Dalton Trans. **43**, 5382 (2014)
21. X. Yi, S. Zhou, C. Chen, H. Lin, Y. Feng, K. Wang, Y. Ni, Ceram. Int. **40**, 7043 (2014)